

Monte Carlo Simulation of 2-D Quantum Gravity as Open Dynamically Triangulate Random Surfaces

E. Adi¹, M. Hasenbusch², M. Marcu³,
E. Pazy¹, K. Pinn⁴, and S. Solomon¹

¹ Racah Institute of Physics
Hebrew University, 91904 Jerusalem, Israel
eti@vms.huji.ac.il
pazy@vms.huji.ac.il
sorin@vms.huji.ac.il

² CERN Theory Division
CH-1211 Genève 23, Switzerland
hasenbus@surya11.cern.ch

³ School of Physics and Astronomy
Raymond and Beverly Sackler Faculty of Exact Sciences
Tel Aviv University, 69978 Tel Aviv, Israel
marcu@vm.tau.ac.il

⁴ Institut für Theoretische Physik I, Universität Münster
Wilhelm-Klemm-Str. 9, D-48149 Münster, Germany
pinn@yukawa.uni-muenster.de

Abstract

We describe a Monte Carlo procedure for the simulation of dynamically triangulate random surfaces with a boundary (topology of a disk). The algorithm keeps the total number of triangles fixed, while the length of the boundary is allowed to fluctuate. The algorithm works in the presence of matter fields.

We here present results for the pure gravity case. The algorithm reproduces the theoretical expectations.

1 Introduction

The quantization of the 2-dimensional Einstein-Hilbert theory of gravity presents conceptual and technical difficulties [1]. In the Euclidean path integral formulation, one has to integrate over all metrics (modulo diffeomorphisms) of a Riemannian manifold with fixed topology. One way of making sense out of this ill defined integral is to approximate the manifolds by triangulations. The integration over all metrics is then replaced by a summation over all triangulations.

The approach to quantum gravity via Dynamically Triangulate Random Surfaces (DTRS) opens the way for the use of Monte Carlo methods which were proven to be very useful, especially if it comes to the inclusion of matter fields [2].

In this letter, we present a Monte Carlo procedure for the simulation of DTRS that have a boundary.

The importance of the boundary comes from the fact that the estimation of the probability distribution of its length corresponds to a measurement of the wave function of the 2D universe. Its theoretical treatment turned out to be problematic. With only the Hilbert-Einstein term in the action, 2-D quantum gravity is non-renormalizable by naive power counting and is known to suffer from ultraviolet divergences. Furthermore, when conformal field theory is coupled to 2-D gravity, a naive counting yields “ -1 ” degrees of freedom [3]. This is believed to reflect a non-normalizable universe wave function solution of the Wheeler-de Witt equations. Matrix model results indicate too that the wave function might be non-normalizable at small areas. These considerations led us to a numerical study of open random surfaces (surfaces with a boundary). The hope is that adding extra boundary terms (or additional matter fields) to the action might lead to a normalizable wave function.

It is therefore useful to have a Monte Carlo algorithm for the simulation of open random surfaces, not only to understand the nature of a possible normalizable wave function but also as a tool to study the intrinsic geometry of open surfaces.

A Monte Carlo procedure for the simulation of closed surfaces with a fixed number of triangles, using the (2,2) Alexander move (to be called “bulk flip” later) was studied by Kazakov et al. [4]. A generalization of this type of algorithm to the case of a surface with a boundary with fluctuating length

turns out to be nontrivial. The main problem is to ensure ergodicity and detailed balance (i.e. that each triangulation contributes with equal probability to the partition function).

This letter is organized as follows. The model is introduced in section 2. Section 3 is devoted to the description of the algorithm. In section 4 we present our results and compare them with the theoretical values.

In the present paper we limit ourselves to the pure gravity case where most of our results can be obtained also analytically. The inclusion of the matter fields (possibly with central charge $c > 1$) where no analytical results are available is straightforward algorithmically, but its theoretical diagnostics and interpretation is beyond the framework of the present letter.

2 The model

The Euclidean Einstein-Hilbert action is

$$S_E[g] = \frac{1}{16\pi G_N} \int_M d^2x \sqrt{|g|} (-R + 2\Lambda). \quad (1)$$

Here G_N is Newton's constant, R is the intrinsic curvature, and Λ is the cosmological constant, in units of $\hbar = c = 1$. M is a Riemannian space time manifold.

In the continuum quantized version (for the sake of completeness we include matter fields X here) one considers the partition function

$$Z = \int \frac{DgDX}{\text{vol}(\text{Diff})} \exp(-S_E[g] - S_m[X, g]). \quad (2)$$

The discrete analog of eq. (2) without matter fields is

$$Z = \sum_{\{\tau\}} \frac{1}{s(\tau)} \exp(a_0 N_0 + a_1 N_1 + a_2 N_2). \quad (3)$$

The sum is over all *oriented* triangulations τ of the surface. N_0, N_1, N_2 are the number of vertices, links and triangles of τ , respectively, and $s(\tau)$ is the order of the symmetry group of the triangulation τ . a_0, a_1, a_2 are free parameters. The factor $\frac{1}{s(\tau)}$ can be viewed as what remains from the $\frac{1}{\text{vol}(\text{Diff})}$ factor in eq. (3).

For open surfaces the action in eq. (2) picks up two additional terms (as in the Liouville theory),

$$S \rightarrow S + \frac{1}{16\pi G_N} \oint_{\partial M} d\hat{s} \sqrt{\tilde{h}} (-k + 4\Xi), \quad (4)$$

where \tilde{h} is the induced boundary metric, k is the extrinsic curvature on the boundary, and Ξ is the boundary cosmological constant.

The Einstein-Hilbert action is a topological invariant, since the 2-D oriented manifolds obey the Gauss-Bonnet theorem (with the correction arising from the boundary term):

$$\frac{1}{4\pi} \left(\int_M d^2x \sqrt{|g|} R + \oint_{\partial M} \sqrt{\tilde{h}} d\hat{s} k \right) = \chi. \quad (5)$$

Here $\chi = 2 - 2h - b$ is the Euler characteristic. h is the number of handles, and b is the number of boundaries. Nevertheless some non-trivial quantum theory exists, mainly due to conformal anomalies [5].

From the topological relation $\chi = N_0 - N_1 + N_2$, and the relation for a connected triangular lattice $2N_1 = 3N_2 + L$, where L is the boundary length, the discrete action in eq. (3) can be written as

$$a_0 N_0 + a_1 N_1 + a_2 N_2 = -\lambda N_2 - \xi L + \gamma \chi, \quad (6)$$

with

$$\begin{aligned} \lambda &= -\left(\frac{a_0}{2} + \frac{3a_1}{2} + a_2\right) \\ \xi &= -\frac{a_0 + a_1}{2} \\ \gamma &= a_0. \end{aligned} \quad (7)$$

The action depends on three independent parameters: λ and ξ , that we identify with the cosmological constants Λ and Ξ , and γ , that we identify with $1/G_N$. Actually as we fix χ , since we identify γ with a constant term, we expect the partition function to look like

$$Z = \sum_{\{\tau\}} \frac{1}{s(\tau)} e^{-\lambda N} e^{-\xi L} = \sum_{N,L} Z(L, N) e^{-\lambda N} e^{-\xi L}. \quad (8)$$

Here and in the following we have identified $N \equiv N_2$.

In our simulations to be specified below one estimates $Z(N, L)$ which is the combinatorial weight of a surface with N triangles and L external edges.

We consider open connected triangulate surfaces without 1- and 2-loops.¹ In the language of the dual lattice, where a triangle becomes a point, an edge a segment and a vertex a polygon, every surface S is in one-to-one correspondence with a connected planar diagram of the ϕ^3 theory without tadpoles and self-energy.

One of our aims is to find the wave function $\psi(L)$, which is the probability amplitude to have a boundary length L , for a *fixed* number of triangles N . Our Monte Carlo procedure samples the configuration space with no a priori weight (each configuration occurs with the same probability). We can therefore determine the probability that a configuration has boundary length L by just making a simple histogram, cf. section 4.

As a by-product of the simulation one gets knowledge about the intrinsic geometry of the surface. Using the simulation results, we are able to picture and characterize the typical surfaces.

3 Algorithm

We consider a connected, open, triangulate lattice, with the topology of a disk. By definition, all edges have equal length. We have to distinguish three types of triangles:

- *type-0* triangles have *none* of their three edges on the boundary of the surface (bulk triangles),
- *type-1* triangles share exactly *one* edge with the boundary,
- *type-2* triangles have *two* edges in common with the boundary.

Our Monte Carlo algorithm generates a start configuration that consists of N triangles and that has a certain boundary length L_0 . Then a number of sweeps is done. Each sweep consists of a sequence of elementary flips done on the configuration:

¹Given a triangulate surface S , a p -loop is a set of p distinct edges in S which form a loop on S

- *bulk flips* change the internal geometry but maintain a fixed boundary length.
- *boundary flips* change the boundary length L . There are two kinds of boundary flips:
 - *type-1 boundary flips* are performed on *type-1* triangles and increase the boundary length by 2.
 - *type-2 boundary flips* act on *type-2* triangles and decrease the boundary length by 2.

Because of the relation $E = \frac{3N+L}{2}$ for a connected triangular lattice, where E is the (integer) number of edges in the configuration, we deduce that for fixed N , the boundary length L may be incremented by even values only.

Let us characterize in detail each of the three flip operations:

- *Bulk flips* (see fig. 1):
These are the basic moves also used in the simulation of closed DTRS [6], see fig. 1.
- *Type-1 boundary flips* (see fig. 2):
One adds a vertex to the configuration and connects it to the two border sites of the *type-1* triangle. The connecting links are called “virtual” edges. One then performs a *bulk flip* on the former border link of the *type-1* triangle. Now one selects one of the two virtual boundary links (each of them with probability one half) and removes it. The remaining virtual link is then made “real”. The so defined operation obviously increases L by 2. Note that the *type-1* flip is allowed only when the resulting configuration is connected.
- *Type-2 boundary flips* (see fig. 3):
To the given *type-2* triangle one adds two virtual links as depicted in fig. 3. Then the *type-2* triangle is removed and, with uniform probability, one of the two virtual links is selected and removed. Finally the remaining virtual link is made real. The *type-2 boundary flip* decreases L by 2.

In order to be able to prove later the detailed balance condition (9), the 3 types of flips have to be applied according to the following prescription.

During the Monte Carlo sweeps one selects again and again with uniform probability one of the N triangles as a candidate for updating.

Once a triangle is selected, one decides what kind of flip will be attempted on it.

Strange as it may look, the constraints of the detailed balance proof (see below) require that the kind of the update (flip) is to be decided *a priori*, independent of the actual type of the triangle on which it is going to be attempted.

More precisely, one decides with probability $0 < p < 1$ to perform a *boundary flip*, and with probability $1 - p$ to perform a *bulk flip* (p is a free parameter which we chose in our runs to be 0.5).²

If the selected update kind is “boundary” and the triangle is *type-0* (“bulk”) then the present updating attempt is aborted and one proceeds to the selection of a new candidate triangle.

If the update kind is “boundary” and the triangle is *type-1* or *type-2* then one applies the corresponding *boundary flip*.

If the update kind is “bulk” one selects with uniform probability one of the three links (edges) of the triangle. If the link belongs to the boundary, the updating attempt is aborted and one proceeds to the selection of a new triangle. Otherwise the selected link is bulk flipped.

In Monte-Carlo simulations one must ensure that the stochastic process is ergodic, i.e., that all configurations can be reached starting from an arbitrary initial configuration.

The ergodicity for fixed N and L comes from the ergodicity of the Alexander (2,2) move (the bulk flip). Therefore all configurations with fixed (N, L) can be reached by a finite number of steps. With boundary flips one can get, for a fixed N , from any L to any \tilde{L} provided that L and \tilde{L} have the same parity and that $3 \leq \tilde{L} \leq N + 2$. These two restrictions are specific for the model that we consider. Thus the combined flips provide an ergodic process for a fixed number of triangles and a varying boundary length.

In order to ensure that each configuration is generated with equal probability we demand that our Monte Carlo procedure satisfies the detailed balance condition. In the absence of matter fields this means that the prob-

²Another flip operation, also consistent with stationarity, is performing bulk and boundary flips in fixed order, e.g., alternating

ability P to move from one configuration to another obeys

$$P(\tau \rightarrow \tilde{\tau}) = P(\tilde{\tau} \rightarrow \tau). \quad (9)$$

It is known that eq. (9) is fulfilled for bulk flips [6]. We therefore consider configurations $\tilde{\tau}$ that differ from τ by a boundary flip. The probability that a certain triangle is selected to be boundary flipped is $\frac{1}{N}$. (Of course, as mentioned above, the triangle will be actually flipped, only if is *not* a *type-0* triangle.) There are four flip possibilities. In each one a couple of triangles $(*,*)$ from τ (where $(*,*)$ expresses the types of the triangles) change their type:

- (1+) a *type-1 boundary flip* changes a $(type-1, type-0)$ combination into a $(type-2, type-1)$ combination. This operation is applied with probability $\frac{1}{2N}$. The factor $\frac{1}{2}$ comes from choosing the neighbour *type-0* triangle out of two possible neighbours of the *type-1* triangle.
- (1-) a *type-2 boundary flip* (also selected with probability $\frac{1}{2N}$) moves a $(type-1, type-2)$ combination to a $(type-0, type-1)$ combination. This is the move depicted in fig. 3. It is the “inverse” operation to (1+).
- (2+) a *type-1 boundary flip* (selected with probability $\frac{1}{N}$) changes a $(type-1, type-1)$ into a $(type-2, type-2)$ combination. This is the operation depicted in fig. 2.
- (2-) The “inverse” operation of (2+) is a *type-2 boundary flip* taking a $(type-1, type-2)$ combination into a $(type-1, type-1)$ combination. It is also selected with probability $\frac{1}{N}$.

The verification of the detailed balance condition is in the statement that the (+) and (-) operations are inverse to each other and are selected with the same probability.

Note that our algorithm can be easily adapted to the inclusion of matter fields (which live on the triangles).

For the actual simulation we used two geometrically very different initial configurations. This enabled us to check the ergodicity of our algorithm and also gave us the possibility to check for critical slowing down. The two initial configurations were:

1. A polyhedron consisting of N triangles, see fig. 4. All triangles are *type-1* and share a single vertex.
2. A configuration that contains 20 *type-1* triangles and $N - 20$ *type-0* triangles. For large N this initial configuration resembles a sphere with a hole in it.

This second initial configuration is constructed by taking a configuration of the first type with $N = 20$ and growing it by inserting vertices in the middle of the triangles [6], see fig. 5. Each vertex insertion increases N by two. After each insertion of a vertex, we performed a sweep.

4 Results

Using the algorithm described above we looked at various quantities. For several different values of N we obtained estimates for the mean of the boundary length ($\langle L \rangle$), and the variance of the boundary length ($\langle L^2 \rangle - \langle L \rangle^2$). We also studied the expectation values of the number of *type-0, 1, 2* triangles and of the number of triangles N_f that do not have any vertex on the boundary.

For thermalization we typically performed 15,000 sweeps. For measurement we typically performed 150,000 sweeps per run (measuring after each sweep).

$\langle L \rangle$ turns out to be a linear function of N with high precision. In table 1 we present our Monte Carlo results for N ranging from 50 to 6400. We give always two estimates for $\langle L \rangle$, one obtained from a run with initial boundary length $L_0 = 20$ and one from a run with $L_0 = N$. The results are always nicely consistent within 1σ error bars. Fitting the data with the law $\langle L \rangle = A + B N$ we find $A = 1.61(3)$, $B = 0.764697(34)$, $\chi^2/\text{dof} = 1.5$ for the data obtained from runs with $L_0 = 20$, and $A = 1.62(3)$, $B = 0.764643(34)$, $\chi^2/\text{dof} = 2.4$ for the data obtained from runs with $L_0 = N$.

The constant B can be obtained analytically: The result for our lattice model is $B = \frac{13}{17} = 0.764706$ [7]. Our fit result from the $L_0 = 20$ runs are nicely consistent with this exact result while the fit to the $L_0 = N$ result is consistent within 2σ .

The linear dependence of $\langle L \rangle$ on N indicates a fractal dimension of the typical equilibrium configuration and the fact that it is composed by loosely connected subgraphs. Further evidence that this is indeed the situation can

be seen in table 2 that quotes the expectation values of the number of triangles not touching the boundary $\langle N_f \rangle$. This data indicates that a typical configuration is tree-shaped with most links belonging to the boundary. Most of the branches look like beads of minimal width (1 link across).

The variance of L goes like $N^{\frac{1}{2}}$. This suggests that the locations of the further branching within a branch are random independent variables. In particular, this implies that there are no long range correlations between the various local geometric features of these “surfaces”.

To obtain further information about the global structure of equilibrium configurations we made some “snapshots” of small N configurations. The “portrait” of such a typical surface (represented on the dual lattice) is shown in fig. 6. This “snapshot” substantiates the picture that the typical surfaces are tree or root like with branching occurring at random walk steps on the configuration.

Fig. 7 shows an example for the statistical distribution of the border length L for $N = 400$ (the wave function $\psi(L)$). The diamonds show the exact result [7], the points with error bars show estimates produced with our algorithm. The error bars were obtained as follows: The total of 100,000 measurements of L was produced in 10 independent runs, each of size 10,000 sweeps. The sweeps consisted of 10,000 flips of each type. A histogram was determined for each subsample separately. The error bars were obtained as the 1σ error from the 10 independent measurements of the histogram.

In conclusion we have presented results from a simulation study of pure 2-D quantum gravity on open DTRS's. The numerical results agree with results obtained by analytical calculations [7]. In addition our simulation algorithm also allowed us to study the geometry of the typical surface configurations.

Our results encourage further advance by adding matter fields.

Acknowledgments

We would like to thank S. Elitzur, T. Mohaupt, T. Wittlich and E. Rabinovici for stimulating discussions.

References

- [1] D. Weingarten, Nucl. Phys. B210 (1982) 229;
R. Friedberg and T.D. Lee, Nucl. Phys. B242 (1984) 145;
for a recent review, see F. David, preprint *hep-th-9303127*.
- [2] C.F. Baillie and D.A. Johnston, Phys. Lett. B286 (1992) 44;
S.M. Catterall, J.B. Kogut and R.L. Renken, Phys. Lett. B292 (1992) 277.
- [3] S. Elitzur, A. Forge and E. Rabinovici, Phys. Lett. B289 (1992) 45.
- [4] V.A. Kazakov, Phys. Lett. B150 (1985) 282.
- [5] A.M. Polyakov, Phys. Lett. B103 (1981) 207.
- [6] D.V. Bultov, V.A. Kazakov, I.K. Kostov, and A.A Migdal,
Nucl. Phys. B275 (1986) 641.
- [7] E. Adi and S. Solomon, in preparation.

List of Tables

1	Monte Carlo estimates for $\langle L \rangle$	12
2	Monte Carlo estimates for $\langle N_f \rangle$	14

List of Figures

1	The bulk flip	12
2	The <i>type-1</i> boundary flip	13
3	The <i>type-2</i> boundary flip	13
4	The polyhedron start configuration	14
5	Growing the initial configuration	14
6	Snapshot of a configuration on the dual lattice	15
7	Probability distribution of L for $N = 400$	16

N	L_0	$\langle L \rangle$
50	20	39.83(5)
50	50	39.78(5)
100	20	78.05(5)
100	100	78.11(5)
200	20	154.54(6)
200	200	154.63(6)
400	20	307.62(8)
400	400	307.45(8)
800	20	613.4(1)
800	800	613.4(1)
1600	20	1225.1(1)
1600	1600	1224.9(1)
3200	20	2448.7(2)
3200	3200	2448.7(2)
6400	20	4895.6(3)
6400	6400	4895.4(3)

Table 1: Monte Carlo estimates for $\langle L \rangle$

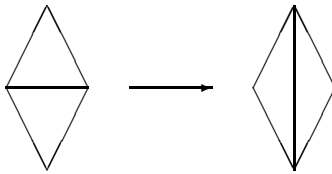


Figure 1: The *bulk flip*

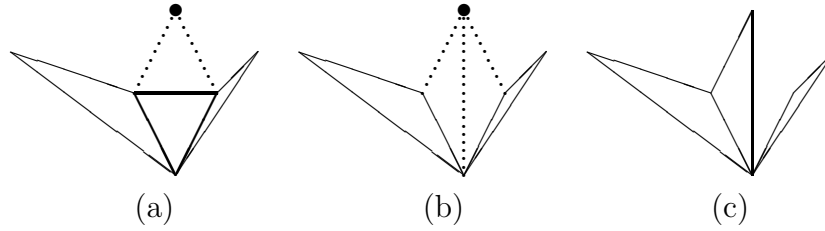


Figure 2: How the *type-1 boundary flip* works: (a) A vertex is added to the configuration and connected to the two border sites of the *type-1* triangle. (b) A bulk flip is performed. (c) One of the two virtual boundary edges is removed. The remaining edges are made real.

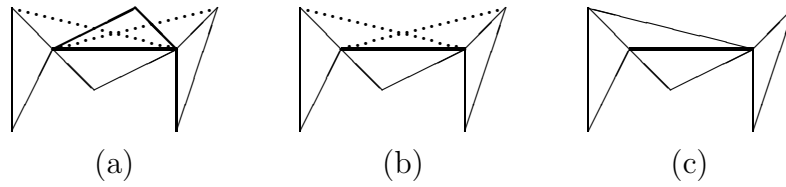


Figure 3: How the *type-2 boundary flip* works: (a) Two virtual edges are added to the configuration. (b) The *type-2* triangle is removed. (c) One of the virtual links is removed, the other is made real.

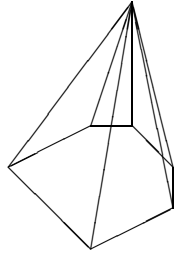


Figure 4: Polyhedron start configuration

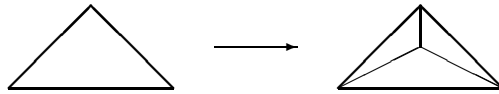


Figure 5: Growing the initial configuration

N	$\langle N_f \rangle$
50	0.51(1)
100	0.96(1)
200	1.92(2)
400	3.85(2)
800	7.67(3)
1600	15.27(5)
3200	30.47(6)

Table 2: Monte Carlo estimates for $\langle N_f \rangle$

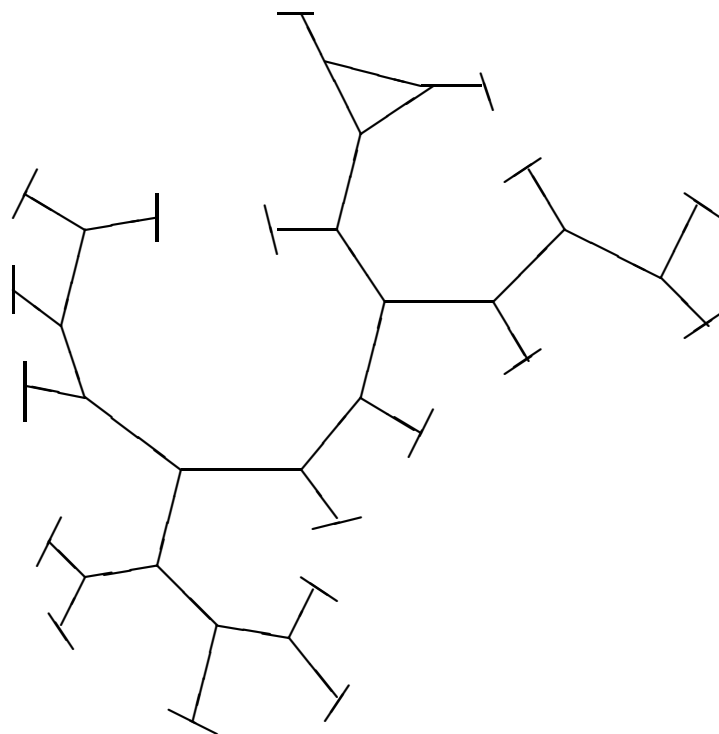


Figure 6: Snapshot of a configuration on the dual lattice

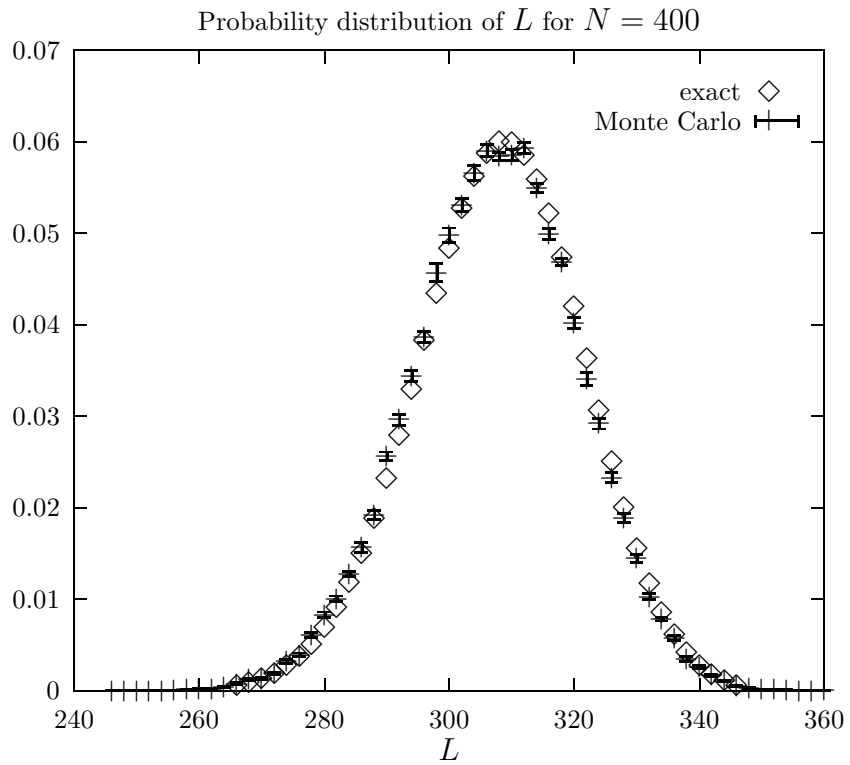


Figure 7: Monte Carlo (points with error bars) and exact results (diamonds) for the wave function $\psi(L)$ for $N = 400$